Power Focusing with Intelligent Reflective Surfaces for Wireless Indoor Communication Systems

MINGYE GONG
MASTER´S THESIS
DEPARTMENT OF ELECTRICAL AND INFORMATION TECHNOLOGY
FACULTY OF ENGINEERING | LTH | LUND UNIVERSITY

Power Focusing with Intelligent Reflective Surfaces for Wireless Indoor Communication Systems

Mingye Gong
mi1377go-s@student.lu.se

Department of Electrical and Information Technology
Lund University

Supervisor: Ove Edfors

Examiner: Fredrik Rusek

March 23, 2021

Printed in Sweden
Tryckeriet i E-huset, Lund

Abstract

Intelligent reflective surfaces (IRS) are envisioned to have a significant number of applications in future wireless network systems by reconfiguring the signal propagation to improve system performance. In particular, the IRS's cell elements can independently reflect the incident signal by tuning its phase and achieving passive beamforming to enhance the received signal of the user equipment. We study the IRS-aided point to point multiple-input single-output (MISO) wireless system where one IRS is deployed to assist the wireless communication network from a multi-antenna base station to a single-antenna user. The user receives the signal transmitted directly from the base station as well as that reflected by the IRS. We aim to maximize the total received signal power at the user by jointly optimizing the (active) transmit beamforming at the base station and (passive) reflect beamforming by the IRS's reflective cells. First, we propose a signal model for the passive IRS-aided wireless network for empty-room and dead-zone scenarios. Second, we propose a beamforming optimization algorithm to analyze the received signal power's maximization for the given scenarios. The performance of the proposed methods is analyzed in an ideal indoor environment where all the antennas both in the base station and the IRS are in a perfect line-of-sight propagation environment. Furthermore, numerical results show significant performance enhancement with the use of IRS in typical wireless networks compared to benchmark schemes. The numerical results show how the IRS-aided wireless system compensates for the attenuation loss blocking by the obstacle wall with different materials in the dead-zone scenarios. Moreover, we present the relationship between the size of the IRS and the received signal power and the size of the IRS and the IRS deploying positions, respectively. It is verified that the IRS can drastically enhance the link quality and coverage over the traditional setup without the IRS.

Acknowledgement

I would like to express my gratitude to my supervisor: professor Ove Edfors for allowing me to conduct my master thesis at Lund University and providing me with valuable suggestions, productive feedback, and guidance during the entire work. I would like to thank professor Harry Leib from McGill University for giving me such an exciting research topic and innovative ideas. I would like to thank all the staff and members from the International office for being kind and supportive through my two years of study at LTH.

Finally, I would like to thank my family and friends for all the support during my study at Lund University.

Table of Contents

List of Figures

Chapter 1

Introduction

1.1 Background and motivation

Intelligent Reflecting surface(IRS) is a brand-new concept providing a revolutionizing technology in wireless communication that will improve the communication network significantly [1]. The IRS will have a substantial potential use in future 6th generation (6G) and beyond wireless networks [2], [3], [4]. The IRS is an artificial meta-surfaces that can control the electromagnetic field on the entire surface, adapt reflecting signals, and proactively modify the wireless channel. IRS differs significantly from the other related existing technologies such as amplify-and-forward (AF) relays, backscatter communication, and active intelligent surface-based massive MIMO [5]. For instance, IRS does not require the use of transmitting RF chains, and it can be densely deployed with scalable cost and low energy consumption [6], [7]. The main advantage of IRS technology is that it enables transmitted power, focusing on a target location while reducing interference to its neighbors [8]. This capability, can, logically, be translated into a significant increase in transmission data rates, without an unrealistic increase in transmission power. All the above advantageous make IRS an appealing solution for performance enhancement in next generation wireless networks, especially for indoor environments with a high density of users (e.g. shopping malls, airports, stadiums). Moreover, IRS has excellent compatibility with existing conventional networks, that is, in existing networks, IRS can be flexibly deployed to enhance the performance of current communication networks. Typical applications of the IRS-aided wireless network are illustrated in [9]. Besides the promising applications shown in [9], IRS also possesses appealing advantages from the implementation aspect, such as lightweight, conformal geometry, and low-cost [9]. However, at this time, the IRS technology is at an infancy stage, and much more research is needed before it can be deployed in practical systems.

1.2 Purpose and aims

The aims of the thesis are analyzing and maximizing the total received signal power at the user equipment by jointly optimizing the (active) transmit beamforming at the base station and (passive) reflect beamforming by the reflective

cells at the IRS. For simplicity, we focus on a single user Multiple-Input-Single-Output (MISO) communication system, aided by an IRS comprising passive reflecting element cells. Deploying an IRS that has set clear links between the BS and user equipment helps bypass the obstacle via intelligent signal reflection in the dead-zone scenario and generates a LoS link between them. This new technology is particularly useful for the coverage extension in mmWave communications that are highly vulnerable to indoor blockage [9], [11]. This thesis can be divided into two parts. In the first part of the thesis, we present a general view of the received power distribution in the empty-room scenario with different deploying positions. In the second part of the thesis, we focus on analyzing how IRS compensates for the power attenuation caused by the obstacle blocking the direct signal propagation link between the base station and the user equipment and how the size and the deploying position of the IRS influence the results.

1.3 Approach and Methodology

To achieve the research objectives, the thesis work started with a literature study. First, we conducted a literature survey about the current situation and trend of 6G under IRS aided system research. Second, a proper signal model is formulated. Then according to the signal model, we develop the joint beamforming algorithm and optimize it base on the different indoor scenarios to maximized the received signal power of the single antenna user. Finally, we use MATLAB to evaluate the model performance and simulate the results under different conditions, such as by applying different sized of the IRS, deploying the IRS at different positions. By analyzing MATLAB results under different scenarios, we are able to find the relationship between optimal received signal power versus varied parameters.

1.4 Main Design Challenges

The IRS design and implementation is at an infancy stage, so there are many challenges from different aspects, such as hardware architecture design and signal processing. In this section, we introduce two main challenges in designing and implementing IRS-aided wireless network, including passive beamforming design and IRS deployment. In this thesis, we consider an IRS-aided wireless communication systems as shown in Figure 1.1, where a multi-antenna Base Station (BS) serves a single antenna user with the help of an IRS, while $\mathbf{H}_1$, $\mathbf{h}_2$, and $\mathbf{h}_1$ denote direct wireless channels between BS and IRS, IRS and a user, and BS and a user, respectively. More specific discussion with 3D geometric setups will be discussed in Section 3.

1.4.1 Passive Beamforming Design

The challenge of designing such passive beamforming by IRS is choosing the phase-shift levels of each elements [9]. In general, the transmit beamforming at

the BS needs to be designed with the phase shifts based on all the BS-IRS, IRS-user, and BS-user channels in order to meet their minimum beamforming gain requirement. In practice, however, IRS's massive passive beamforming gain is achieved at the expense of more overhead for channel estimation because of the additional channels involved between the IRS and its associated users [10]. Moreover, wireless networks such as 5G, generally operate in wideband channels with frequency selectivity. Active BS can use digital processing in the frequency domain to deal with the frequency-selective channel variation [12], however, it is challenging to implement passive IRS that are frequency dependent [9].

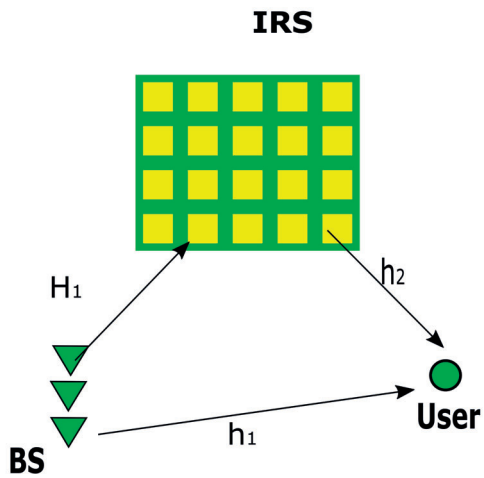

Figure 1.1: An IRS-aided wireless system.

1.4.2 IRS deployment

How to deploy the IRS in the practical indoor environment to optimize the hybrid wireless network performance is another challenge to be solved. As shown in Figure 1.1, the IRS should be intuitively deployed at a position with LoS propagation from the BS to maximize its received signal power for passive beamforming. At the same time, the deployment methods mentioned above may not work well when the IRS needs to simultaneously support transmissions between the BS and the users under their coverage region. The reason behind that is explained in [6]. In this thesis (Section 5) we will take a closer look at this problem.

1.5 Literature review

Prior works on IRS-aided wireless communication can be found in [5], [6], [9], [13]. The design of the IRS parameters for various communication objectives are elaborated in [1], [15]- [18]. The simulation results show the SNR improvement and signal coverage extension achieved by deploying the IRS-aided wireless communication networks as compared to that of the conventional wireless network without IRS [6]. In [14], [19], the role of IRS with passive elements for improving indoor coverage is analyzed. Potential use of the IRS are briefly discussed in [9], [20]. Some theoretical beamforming optimization methods have been discussed in [5], [6], [21], where the results mainly simulated in 2D space and a Zero-Forcing (ZF) precoding method have been used. With the aforementioned discussion in mind, it has not yet been thoroughly investigated the relationship between the deployment position of the IRS and the size of the IRS elements in the Dead-Zone scenario in a 3D indoor environment. Since the majority of literature assume that the BS possesses full Channel State Information (CSI), we make the same assumptiuon throughout the thesis.

1.6 Thesis Outline

The outline of this thesis is as follows: Chapter 2 introduces the theoretical concepts of beamforming technology and Precoding Methods; The system model is demonstrated in Chapter 3. Chapter 4 describes the designing problem. The simulation results of the IRS-aided wireless network by using numerical methods are presented in Chapter 5. Finally, the conclusion and future work are summarized in Chapter 6.

Chapter 2

Technical Background

2.1 Beamforming Technology

Beamforming is one of the key technologies in wireless communication technology. To be specific, beamforming technology is a communication technology that dynamically transforms a transmit beam into a narrower transmit beam in real time at the transmitting end to direct energy to a specific target user and obtain additional system gain, thereby improving the signal quality of the specific target user. Beamforming technology has the following significant advantages [22], [23]:

1. Longer coverage distance: The wireless unit power is unevenly distributed in space. The main radiated energy only points to the location of the terminal to avoid waste of power, improve the overall system gain, and expand the coverage distance.
2. Stronger interference suppression ability: Based on the unbalanced power distribution, the antenna element is pointed at the terminal of the transmitter at the location of the terminal, and the interference to other wireless systems is reduced to the greatest extent possible.

Overall, due to the improvement of the received signal quality of the system and the higher signal-to-noise ratio due to the minimum interference, the system can work robustly at a higher-order modulation method. Beamforming technology can be generally divided into two implementation schemes: fixed weight beamforming and adaptive beamforming [24], [25]. Fixed weight beamforming means that the beam weight vector in the system is fixed, that is, the directional pattern of each antenna is fixed. These fixed beams can form different beam weight vector combinations. The base station selects different combinations and transmits them at the receiving end. Through the beam search method, the combination in which the received signal-to-noise ratio is maximized is selected for communication [26]. Conversely, adaptive beamforming element weights that depend on the signal environment via adaptive algorithms. Adaptive beamforming techniques dynamically adjust the array pattern to optimize some characteristics of the received signal, resulting in the main lobe focusing on the desired signal's arriving direction and suppressing the interfering signal [27]. In practice, when selecting a proper adaptive beamforming algorithm, robustness, complexity, and convergence speed are the main factors to be considered [27].

2.2 Precoding Methods

The use of precoding technology in multi-purpose wireless communication systems can greatly increase the channel capacity of wireless communication and ensure the reliability of signal transmission [28]. From an implementation perspective, precoding algorithms for space-division multiple access (SDMA) systems can be sub-divided into linear and non-linear precoding types [29]. The non-linear precoding methods usually result in a capacity-achieving performance, while the linear precoding approaches usually achieve resonable performance with much lower complexity [30]. Linear precoding strategies include maximum ratio transmission (MRT), zero-forcing (ZF), and transmit Wiener precoding [31], [32]. The benefits mentioned above can be attained by applying simple linear precoding at the transmitter such as transmit-maximal ratio combining (transmit-MRC), zero-forcing (ZF) [3], [33]. Non-linear precoding may be designed based on the concept of dirty paper coding (DPC), which shows that any known interference at the transmitter can be subtracted without the penalty of radio resources if the optimal precoding scheme can be applied on the transmit signal [29], [30]. However, the computational complexity of taking DPC operations is high, and the hardware implementation is particularly difficult, so its practical applications are few [34]. Exploiting spatial diversity in the wireless system with multiple antennas at the BS requires that the transmitted signal be pre-coded prior to transmission [28], and the need for pre-processing the transmit signal is detailed explained in [31], [35].

Chapter 3

System Model

The studied geometric setup, using Cartesian coordinates, is shown in Figure 3.1. Overall, the IRS is placed between the BS and the user, we assume the operating frequency under this setup is 5GHz and λ is the corresponding wavelength. The base station has L antennas and placed linearly in the z-direction, and we denote the position of the ℓ_{th}antenna at base station as $(x_l^{BS}, y_l^{BS}, z_l^{BS})$ where $\ell = 1, 2 \dots L$. The antennas are d_{BS} meters away from each other. The IRS is placed parallel to the $z - y$ plane, and we denote the position of each cell as $(x_{m,n}^{IRS}, y_{m,n}^{IRS}, z_{m,n}^{IRS})$, where $m = 1, 2 \dots M$ and $n = 1, 2 \dots N$. The adjacent cells in IRS are $d_{\text{IRS-h}}$ and $d_{\text{IRS-v}}$ meters apart in horizontal and vertical direction respectively. In this thesis, we narrow down to a single mobile user and the position of the user is denoted by $(x_{user}, y_{user}, z_{user})$. The discrete-time signal received at the mobile user can be expressed as

$$y = (\mathbf{h}_2 \mathbf{\Phi} \mathbf{H}_1 + \mathbf{h}_1)\mathbf{w}s + n, \tag{3.1}$$

where $\mathbf{h}_2 \in \mathbb{C}^{1 \times MN}$ denotes the wireless channel between the IRS and the user, $\mathbf{H}_1 \in \mathbb{C}^{MN \times L}$ denotes the wireless channel between the BS and IRS, $\mathbf{h}_1 \in \mathbb{C}^{1 \times L}$ denotes the direct channel between BS and the user, $\mathbf{\Phi} \triangleq \text{diag}\,[\phi_1, \phi_2, \dots \phi_R]$ with $R \triangleq M \cdot N$ is a diagonal matrix representing the effective phase shifts by all IRS elements, $\mathbf{w}_k$ and $s \in \mathbb{C}^{MN \times 1}$ denote the precoding vector and information symbols which are modeled as in dependent and identically distributed (i.i.d) random variables with zeros mean and unit variance, respectively, while $n_k \sim \mathcal{CN}(0, \sigma^2)$ represents the thermal noise power at the receiving user. Accordingly, the signal power received at the user is given by

$$\gamma = \left\| (\mathbf{h}_2 \mathbf{\Phi} \mathbf{H}_1 + \mathbf{h}_1)\mathbf{w} \right\|^2. \tag{3.2}$$

For analytical tractability, we assume that the reflected signals will be absorbed when they touch the ceiling, floor, and walls of the indoor environment except for the IRS, and a perfect line-of-sight propagation between the base station and IRS, and IRS and the user equipment will be considered. The distance d_{BS}, $d_{\text{IRS-h}}$ and $d_{\text{IRS-v}}$ are chosen as $\lambda/2$. Therefore, channel $\mathbf{h}_1$, $\mathbf{h}_2$, and $\mathbf{H}_1$ can be characterized as follows,

$$\mathbf{h}_1(l) = \frac{\lambda}{4\pi d_{B_{(l)}U}} e^{\frac{-j2\pi d_{\text{B}_{(l)}\text{U}}}{\lambda}}, \tag{3.3}$$

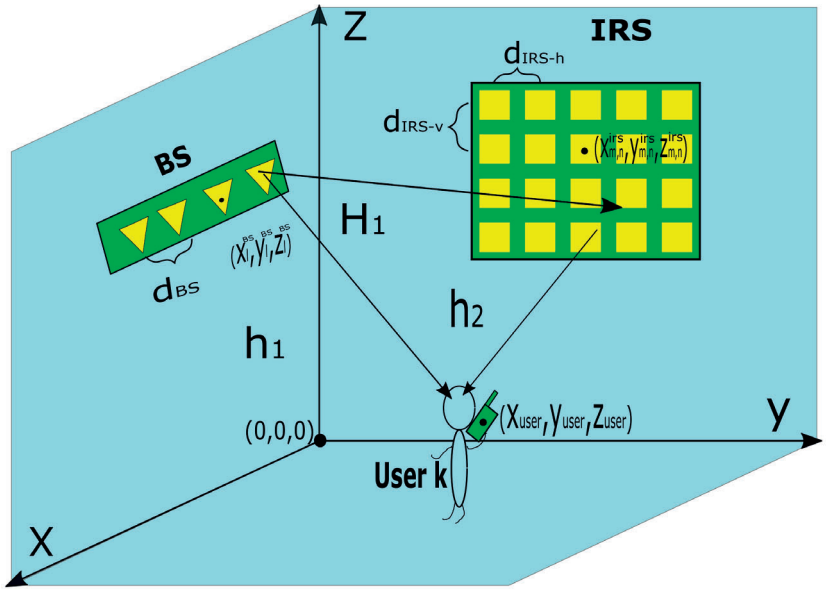

Figure 3.1: A general view of the geometric setup in 3D.

$$\mathbf{h}_2(m \cdot M + n) = \frac{\lambda}{4\pi d_{\mathrm{I}_{(m,n)}\mathrm{U}}} e^{\frac{-j2\pi d_{\mathrm{I}_{(m,n)}U}}{\lambda}}, \tag{3.4}$$

$$\mathbf{H}_1(m \cdot M + n, l) = \frac{\lambda}{4\pi d_{\mathrm{B}_{(l)}\mathrm{I}_{(m,n)}}} e^{\frac{-j2\pi d_{\mathrm{B}_{(l)}\mathrm{I}_{(m,n)}}}{\lambda}}, \tag{3.5}$$

where $d_{\mathrm{B}_{(l)}\mathrm{U}}$, $d_{\mathrm{I}_{(m,n)}\mathrm{U}}$, $d_{\mathrm{B}_{(l)}\mathrm{I}_{(m,n)}}$ represent the Euclidean distance between the l-th antenna at the base station and user, the m-th row and n-th column of the IRS element and the user, the l-th antenna at at base station and the m-th row and n-th column of the IRS, respectively. In this thesis, we consider the IRS can only tune its phase to achieve passive beamforming. Therefore, the effective phase shift by IRS elements is formulated as

$$\phi_r = \alpha e^{j\theta_r} \quad for \;\; r = 1, 2 \ldots R, \tag{3.6}$$

where $\theta_r \in [0, 2\pi]$ is the phase rotation for the r-th cell in the IRS, and α is the power loss factor of the IRS. In paper [36], numerical simulations show that the power efficiency of an inhomogeneous reflective surface is around 94%. In practice, we consider the IRS in our thesis is tunable with considerable transmission loss. Therefore, we consider $\alpha = 0.3$, such that our IRS's power efficiency is about $1/10$ of that number [36].

Chapter 4

Problem Formulation

In this thesis, we consider a single user MISO communication system aided by an IRS comprised of passive reflecting element cells and full knowledge of the CSI at the BS. We denote the total channel presented in (3.1) as

$$\mathbf{H}_{\text{tot}} = \mathbf{h}_2 \mathbf{\Phi} \mathbf{H}_1 + \mathbf{h}_1. \tag{4.1}$$

To exploit spatial diversity, the signal from each antenna at BS is transmitted after being weighted, so that the signal arrive in phase at the IRS and the user added coherently. In order to maximize the received signal power at the user with signal antenna equipment, the problem becomes

$$arg \max_{\mathbf{\Phi},\mathbf{w}} \left|y\right|^2 \Leftrightarrow arg \max_{\mathbf{\Phi},\mathbf{w}} \|\mathbf{H}_{\text{tot}}\mathbf{w}\|_F^2, \tag{4.2}$$

where $\|\cdot\|_F$is the Frobenius norm.

Clearly, the precoding vector $\mathbf{w}$ that maximizes the received SNR can be achieved by applying the maximal ratio combining (MRC) [31], [35].

Thus, the performance optimization of the IRS-aided wireless system problems becomes the maximization of the norm of the total channel. Since we assume the channel knowledge is known at the base station, the only variable here is phase rotation vector Φ. The optimization problem in (4.2)can be formulated as follows,

$$(\mathbf{P1}): \max_{\mathbf{\Phi}} \ f(\Phi), \tag{4.3}$$

where $f(\Phi) = \|\mathbf{H}_{\text{tot}}\|_F$.

Here, we provide two independent constraints for (4.3), which presents as follow,

$$\left|\phi_r\right|^2 = \alpha^2, \ \ for \ \ r = 1, 2, \ldots R, \ \ and \tag{4.4}$$

$$\sum_{r=1}^{R} \left|\phi_r\right|^2 \leq \alpha^2 M \cdot N, \tag{4.5}$$

where (4.4) and (4.5) are two constraints denoted as phase-only-adapted and energy-normalized, respectively. Note that when analyzing the IRS-aided wireless network performance, we either apply (4.4) or (4.5). Intuitively, optimizing **P1** with the (4.5) will outperform than that with (4.4). However, the computational complexity is different between these two linear constraints. Hence, in the next sections, we will apply a numerical method to compare the network performance between (4.4) and (4.5), and we need to find out the number of iteration to guarantee we obtain the global minimum in both constraints. To achieve optimal simulating performance, we apply the numerical method for finding the optimized phase rotation by maximizing the system's gain $\|\mathbf{H}_{\text{tot}}\|_F$ shown in (4.1). We will also analyze wireless network performance of different indoor scenarios by applying the transmit-maximum ratio combining (transmit-MRC) and the optimized phase rotation vectors.

Chapter 5

Simulation results and analysis

In this section, the simulation results of IRS-aided wireless systems of different geometric setups are provided. In order to achieve optimal simulating performance, we apply the numerical method using iterative optimization technique to find the optimized phase rotation by maximizing the system's gain $\|\mathbf{H}_{\text{tot}}\|_F$. This section is divided into three subsections: Subsection 5.1 is mainly discussing the wireless system performance in the empty-room scenario. Section 5.2 presents the wireless system performance in the dead-zone scenario. In Section 5.3, the relationship between the received signal power and the total travel distance of the BS and the user are analyzed. For quantitating how much power gained by applying IRS-aided wireless network, we define the power gain of the IRS aided system as follows:

$$\text{Power Gain (dB)} = 10\log_{10}\left(\frac{P_{\text{IRS+BS}}}{P_{\text{BS}}}\right), \tag{5.1}$$

where $P_{\text{IRS+BS}}$ is the received signal power of IRS-aided system and P_{BS} is the received signal power of traditional base station system. According to the MISO assumptions in the previous section, the definition in (5.1) can be simplified as

$$\text{Power Gain (dB)} = 10\log_{10}\left(\frac{\|\mathbf{h}_2\mathbf{\Phi}\mathbf{H}_1 + \mathbf{h}_1\|_F^2}{\|\mathbf{h}_1\|_F^2}\right). \tag{5.2}$$

We also define the relative received signal power in [dB] as follows,

$$\text{Relative received signal power (dB)} = 10\log_{10}\left(\frac{P_{\text{rx}}}{P_{\text{tx}}}\right), \tag{5.3}$$

where P_{rx} and P_{tx} denote as the received and transmitted signal power, respectively. For simplicity, we consider the transmitted power is normalized to unit one and do not consider any additional noise in this thesis. Note that, since we assume the transmitted power is one for following simulations, we denote the relative received power also as received signal power in the following sections.

In the rest of the sections, we will present the simulation results of the power gain defined in (5.2) for Empty-Room and Dead-Zone Scenarios as defined in

Section 5.1 and 5.2 and also apply a numerical method with different constraints to find the optimized ϕ_r such that to enhance the performance of IRS-aided wireless system. In each scenario, we "optimize" the phase rotation across the surface to see how much it can improve the situation (improved received power), given that the transmit power is kept constant, and "co-optimize" the beam-former at the BS with the phase rotations across the surface, for maximal received power. Comparing this with the results and show that how much power gained by an optimal IRS in both scenarios.

5.1 Empty-Room Scenario

Two vertical views of the empty-room scenario with different geometric setups are presented in Figure 5.1. In particular, we consider the size of the room is 50×50 in meters and the base station is placed at the center of the south wall for all geometric setups. The IRS is placed on the north wall in Figure 5.1a and on the west wall in Figure 5.1b respectively. For these two geometric setups: $d_{\text{bs}} = d_{\text{irs}} = 25$ meters; the base station and the IRS are 3 meters above the ground measured at the geometric center of each component; the height of the user z_{user} is 1.8 meters.

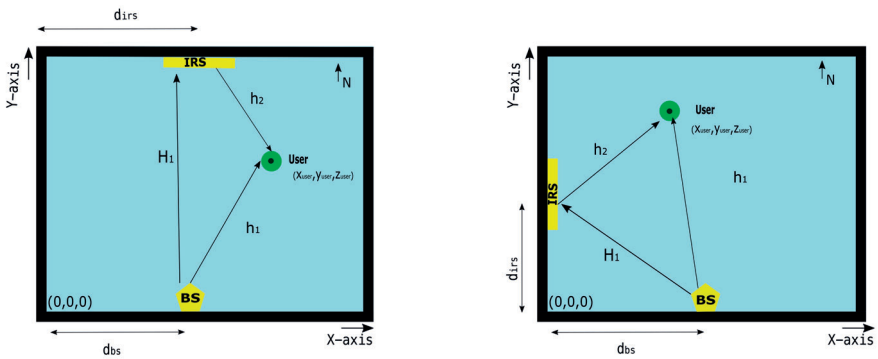

(a) An IRS is deployed on the north wall

(b) An IRS is deployed on the west wall

Figure 5.1: Two vertical views of the empty-room scenario geometric setup.

The simulation results are presented under the condition that the room is empty where both signal propagation links of BS and IRS, IRS, and the user, BS, and user are under LoS. To further improve the performance of the IRS-aided wireless network, the numerical beamforming method (mentioned in Section 4) is applied to iteratively optimize the phase rotation vector. Hence, we should find the minimum number of iteration such that guarantees the **P1** to achieve the optimized phase rotation vector $\mathbf{\Phi}$. Since we have the two independent constraints, the

phase-only-adapted (4.4 and energy-normalized (4.5), we need to analyze them separately. First, let's consider **P1** with the constraint (4.4). In particular, we consider the user moving parallel to the south wall (x-axis) from the left to the right and the vertical distance between the user k and the south wall is always 30 meters. Here, we assume $L = M = N = 8$ and $\alpha = 0.3$.

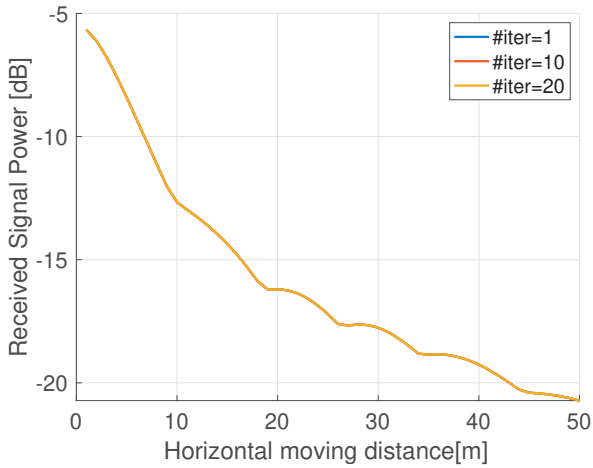

Figure 5.2: Received signal power versus the horizontal distance in x-axis for different numbers of iteration with constraint (4.4).

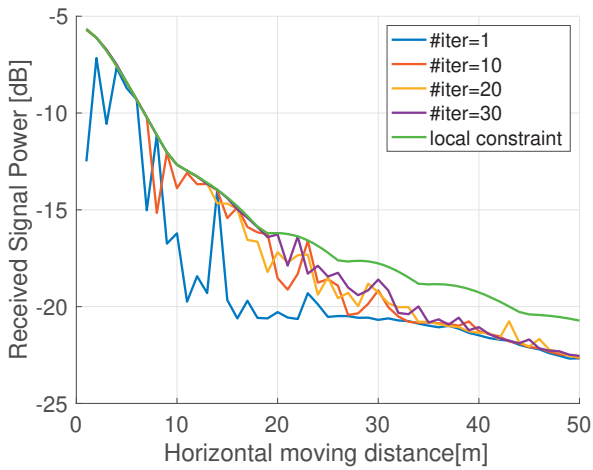

Figure 5.3: Received signal power versus the horizontal distance in x-axis for local constraint (4.4) and different numbers of iteration with constraint (4.5).

As shown in Figure 5.2, the received signal powers with constraint (4.4) are equal for different number of iterations from $\#iter = 1$ to $\#iter = 20$. Although the results of (4.5) are more in line with the practice, constraint (4.5) turns out to be questionable from IRS implementation point of view and with higher computational complexity. While Figure 5.3 shows that, as the number of the iteration increase, the received signal power converges to a certain level, and that level is the received signal power output with the constraint (4.4) shown in Figure 5.2. Hence, for computational simplicity, we apply phase-only-adapted constraint (4.4) with $\#iter = 1$ for the Section 5.1 and Section 5.2.1. Note that, the convergence property may change for more complicated setups and movement. In general, we will get better results when we increase the number of iteration. For improving the simulation performance, the number of the iteration will increase accordingly in Section 5.2.2 and Section 5.3.

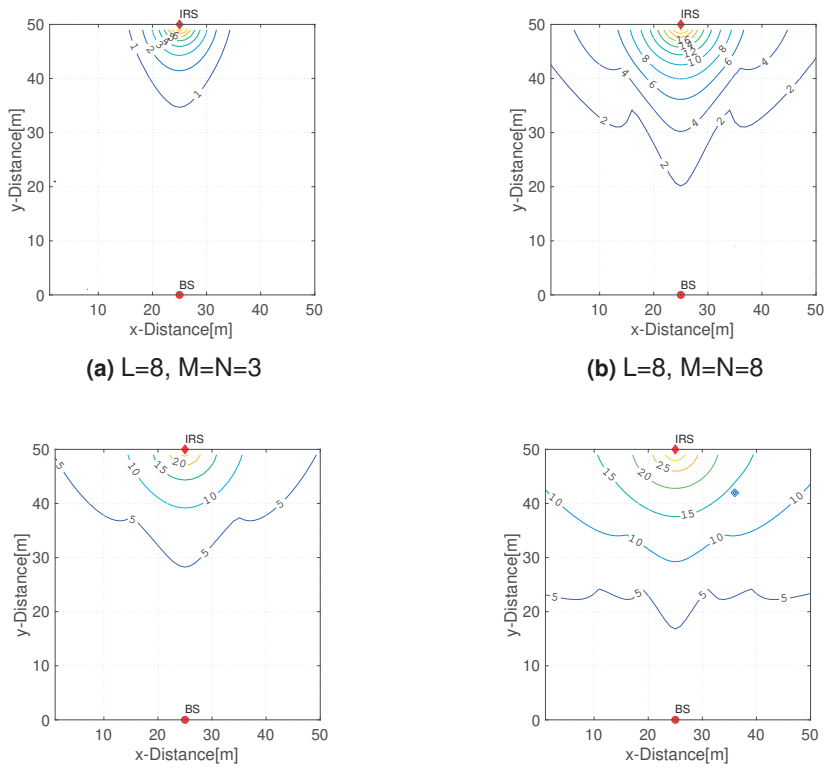

(a) L=8, M=N=3 **(b)** L=8, M=N=8

(c) L=8, M=N=10 **(d)** L=8, M=N=16

Figure 5.4: Contour plot of system power gain in dB for the geometric setup in Figure 5.1b with IRS size of 3×3, 8×8 10×10, and 16×16.

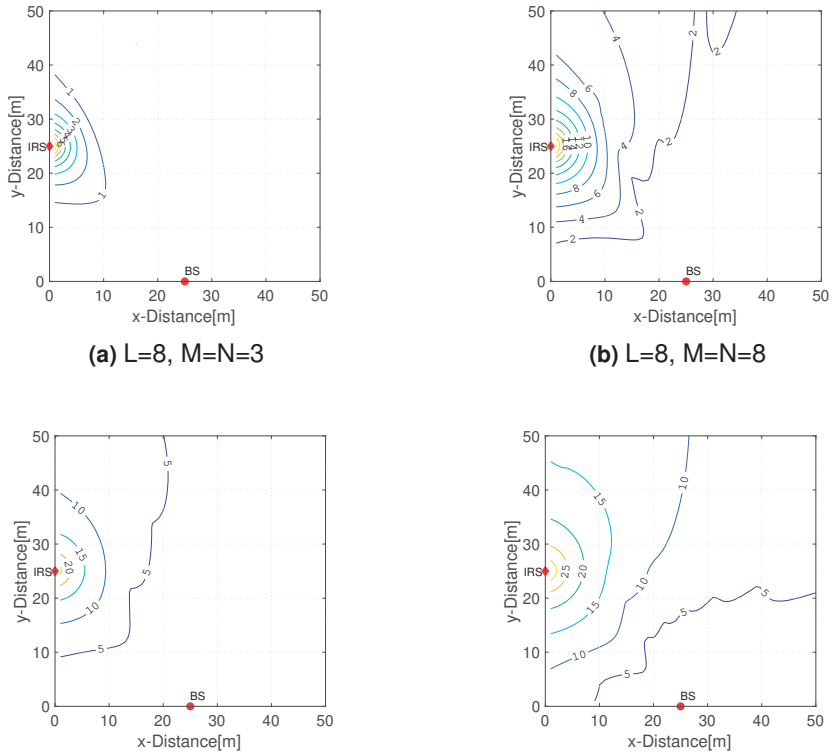

(a) L=8, M=N=3

(b) L=8, M=N=8

(c) L=8, M=N=10

(d) L=8, M=N=16

Figure 5.5: Contour plot of system power gain in dB for the geometric setup in Figure 5.1a with IRS size of 3×3, 8×8 10×10, and 16×16.

Figure 5.4 and Figure 5.5 present the power gain in dB of different setups in the empty-room scenario. We consider the BS is placed at the center of the south wall (x-axis) for both cases, and an IRS is deployed on the center of the north wall in Figure 5.4 and on the center of the west wall in Figure 5.5. Comparing with the traditional wireless network, Figure 5.4 and Figure 5.5 illustrate that there is a significant improvement of power gain for IRS-aided network. The closer to the IRS, the more power gain we can obtain. We can clearly observe the beam structure of the distribution of the power gains from four subfigures in Figure 5.4. For example, in Figure 5.4a, the main lobe is facing directly to the BS, and as M and N increase, side lobes occurs symmetrically around the main lobe shown from Figure 5.4b to Figure 5.4d. In Figure 5.5, the main lobe of the IRS is in the direction that facing towards to the BS, which we can clearly see from Figure 5.5a. This is because in this direction, it creates the shortest wireless link with highest signal energy. There is not much power to gain cover in the northeast corner when

the size of the IRS is $M = N = 3$ shown in Figure 5.5a . As M and N increase, the larger power gain gradually covers northwest region of the space, which can be seen from Figure 5.5b to Figure 5.5c. When the size of the IRS increases to $M = N = 16$ in Figure 5.5d, the power gain on the geometric diagonal of the room is between 5 to 10 dB, and its coverage is far more better than that in Figure 5.4d. However, in Figure 5.1a if there is an obstacle blocking the direct LoS link between the IRS and the BS in , the power gain will be reduced due to the attenuation loss through the obstacle. Hence, the geometric setup in Figure 5.1a is not practical.

Overall, we could see from Figure 5.4 and Figure 5.5 that the power gain of two geometric setups increase as the number of the IRS increases. In the next section, we will focus on the geometric setup in Figure 5.1b and discuss its performance for dead zone scenario.

5.2 Dead-Zone Scenario

5.2.1 Signal power distribution and power gain

The vertical view of the dead-zone scenario is shown in Figure 5.6. We consider a room of size 50×50 in meters and there is an obstacle wall to separate the entire space into two small rooms denoted as room 1 and room 2, respectively. User k is located in room 1 where the direct link between it and its serving BS is severely blocked by an obstacle. In this case, deploying an IRS helps the signal bypass the obstacle via IRS reflection. The base station is placed at the south wall (x-axis) and the IRS is placed the west wall (y-axis). d_{bs}, d_{irs} and d_{w} denote the horizontal distance between the original point and the base station denotes, the vertical distance between the original point and the IRS, and the horizontal distance between the west wall and the left side of the solid wall respectively. The base station and the IRS are all 3 meters above the ground measured at the geometric center of each component and we assume the height of the user z_{user} is 1.8 meters. We denote the maximum horizontal distance between the user and the west wall for a given vertical distance y_{user} is d_1, such that the user can received the LOS signal directly from the base station. When the horizontal position of the user $x_{user} \leq d_1$ for the given vertical distance y_{user}, the user is L0S to the BS + IRS reflection region. when $x_{user} > d_1$ for the given vertical distance y_{user}, the user can received the signal from the IRS's reflection as well as the signal from the base station through the obstacle with a attenuation loss factor β. In this subsection, we consider the obstacle as a glass window and the signal power strength attenuates around 7dB according to Table 5.1 [37].

In particular, we consider $d_{\text{bs}} = 10m$, $d_{\text{irs}} = 30m$, $l_2 = 20m$, $\alpha = 0.3$, and $\beta = \sqrt{10^{-7/10}}$. Since we are interested in the situation that the user is located in the dead zone, we present the power gain defined in (5.2) only at Room 1.

Obstacle	Width (mm)	5GHz Signal Attenuation (dB)
Synthetic material	20	3
Asbestos	8	4
Wooden door	40	4
Glass window	50	7
Heavy colored glass	80	10
Brick wall 1	120	20
Brick wall 2	240	25
Armored glass	120	35
Concrete	240	30

Table 5.1: Attenuation of typical obstacles.

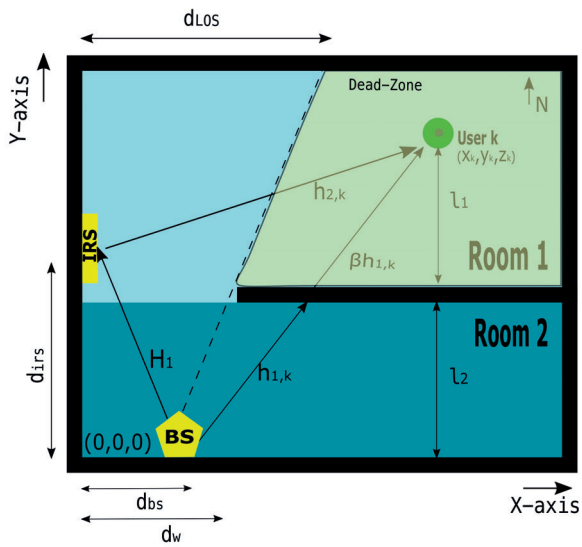

Figure 5.6: The vertical view of the Dead-Zone scenario geometric setup.

Figure 5.7 shows that contour plot of the system power gain of the dead-zone scenario in Room 1. We set the number of the antenna $L = 8$ at the base station and present the power gain with different IRS size. Overall, the power gain increases when the user is close to the IRS as the number of the IRS size increases. Instead of installing an additional BS, the results show that the signal coverage can be extended by deploying an IRS. For example, as we can see from Figure

5.7a, there is nearly no power gain behind the wall in Room 1 when $M = N = 3$ comparing with that when $M = N = 10$, where the power gain distribution increase dramatically. We also observe that the power gain distribution is denser when the user closed to the left side of the dot boundary line. This is because the user received signal is dominated by the BS-user direct link in the left side of the dot boundary line region. According to [5], the received signal power scales with the number of reflecting elements $N \times M$ in the order of $(N \times M)^2$. For example, when we compare the power gain between Figure 5.7b and Figure 5.7d, the power gain at the same position increase around 12dB as the the number of reflecting elements increase 16 times from $8 \times 8 = 64$ to $16 \times 16 = 256$.

So far, we already have the general view of how much the IRS aided system improves the signal strength. In the next subsection, we will analyze the relationship between the size of the IRS and power loss compensation in the dead zone scenario where the user is blocked by the obstacle.

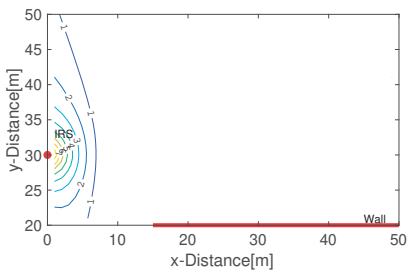

(a) $L = 8$, $M = N = 3$

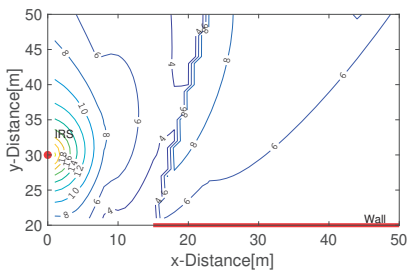

(b) $L = 8$, $M = N = 8$

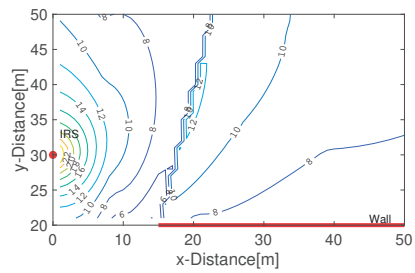

(c) $L = 8$, $M = N = 10$

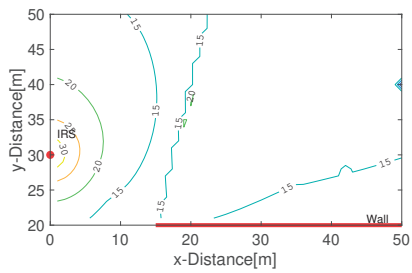

(d) $L = 8$, $M = N = 16$

Figure 5.7: Contour plot of system power gain in dB for the geometric setup in Figure 5.6 with 7dB attenuation loss and different IRS sizes.

5.2.2 Dead-Zone power compensation

The general view of the power gain distribution of the IRS aided wireless system with the indoor solid wall scenario has been shown in section 5.2.1. In this section, we will fix the user position and analyze the relationship between the size of the IRS and received signal power compensation with different deploying positions and different blocking obstacle materials.

Two vertical views of the Dead-Zone power compensation geometric setups presented in Figure 5.8 and Figure 5.13, respectively. In each scenario, we provide two different observation views, known as the wireless channel perspective and the signal coverage perspective. Similarly to the geometric setups of the Empty-Room scenario, we also have two sub-scenarios, where an IRS is deploying at the west wall shown in Figure 5.8 and at the north wall shown in Figure 5.13. The difference between two geometric setups, Empty-Room and Dead-Zone power compensation, is that there is an obstacle blocking the LoS propagation link between the user and the BS. Therefore, the user received the signal power from the BS with a quite large attenuation loss. In this case, deploying an IRS that has clear links with the BS and user helps bypass the obstacle via intelligent signal reflection and thus creates a virtual LoS link between them. This is particularly useful for the coverage extension in mmWave communications and the received signal power compensation that are highly vulnerable to indoor blockage.

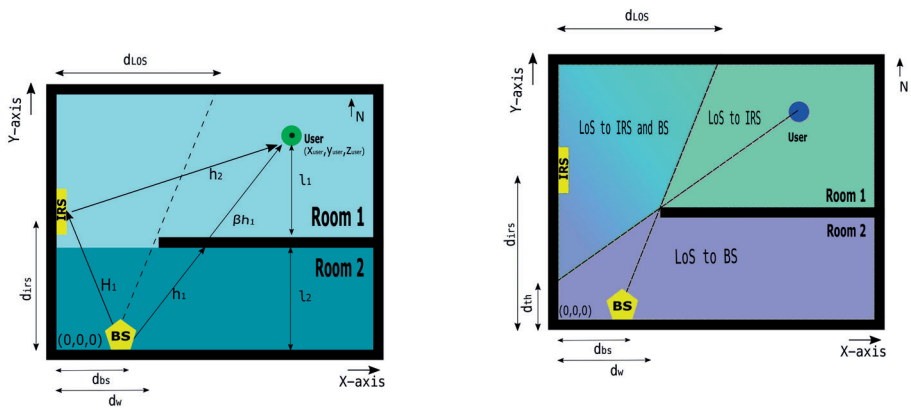

(a) Wireless channel perspective

(b) Signal coverage perspective (From User point of view)

Figure 5.8: Vertical views of the Dead-Zone power compensation scenario geometric setup where IRS is placed on the west wall.

First, we discuss the power performance of the scenario which is shown in Figure 5.8, where an IRS is deployed at the west wall. Figure 5.8a presents the detail geometric setups with wireless channel information, while Figure 5.8b provides

a clear view of the BS and the user's coverage region. We are keeping the same geometric setups as in the section 5.2.1, which means $d_{\text{bs}} = 10m$, $d_{\text{irs}} = 30m$, $l_2 = 20m$, $\alpha = 0.3$. We change the power attenuation factor of the obstacle wall β by selecting different obstacle materials from Table 5.1 for the following simulations. We consider a fixed $l_1 = 20m$, the vertical distance between the user and the obstacle wall, such that the user at $(40, 40, 1.8)$ in the given coordinate system. The user receives the signal is mainly from the IRS and receives a little signal from the base station through the office glass wall with an attenuation loss. The IRS's deploying position is moving along the west wall. In this section, we assume the passive elements of the IRS are distributed as a square structure such that $M = N$, and we defined IRS size as the side length M.

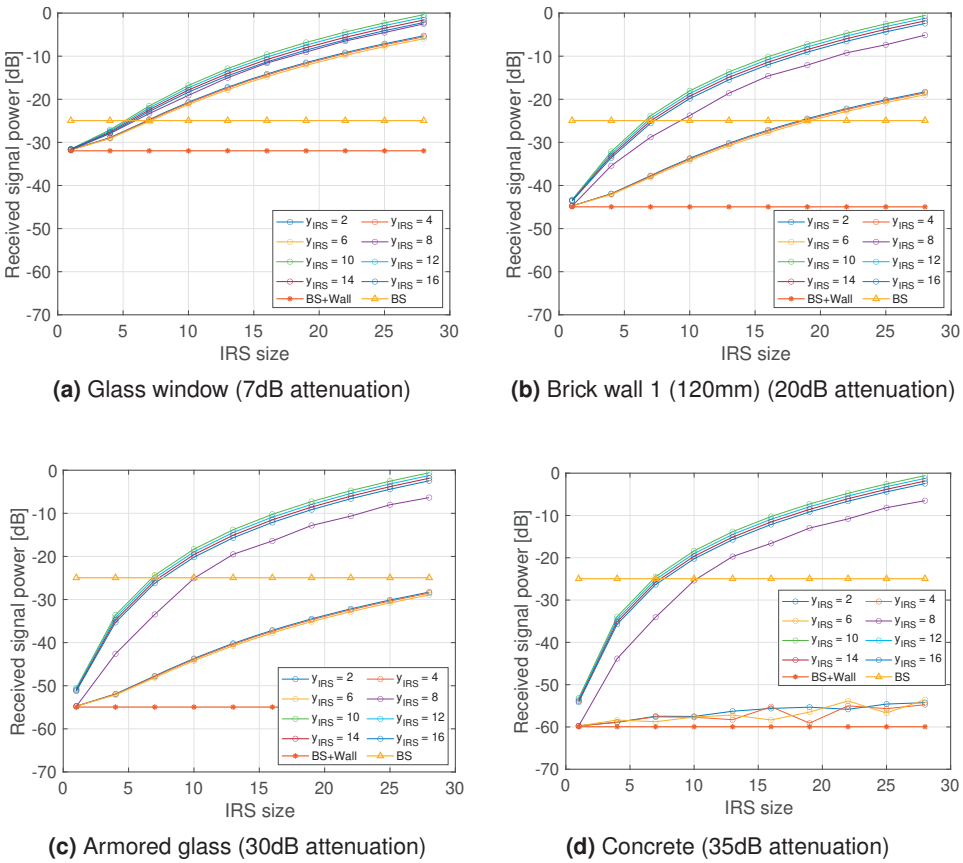

(a) Glass window (7dB attenuation)

(b) Brick wall 1 (120mm) (20dB attenuation)

(c) Armored glass (30dB attenuation)

(d) Concrete (35dB attenuation)

Figure 5.9: Relationship between size of IRS (side length M) and received signal power for four different wall loss attenuation and different IRS deployment positions from $y_{\text{irs}} = 2$ to $y_{\text{irs}} = 16$ on the west wall when $L = 8$.

Figure 5.9 presents the relationship between the size of the IRS and the received

signal power for different IRS deployment positions and different obstacle materials. The yellow triangular dotted line in the middle denotes the received power of the user when the room is empty without any obstacle blocking the user from the BS, and the bottom red triangular dot line denotes the received power of the user when there is an office wall blocking the direct link between the base station and the user, while the curves between them denote the corresponding received power of the user with different IRS deploying position when there is an office wall blocking the direct link between the base station and the user. The deploying position of the IRS is moving along with the west wall shown in Figure 5.8b, where it varies from $y_{\text{irs}} = 2$ to $y_{\text{irs}} = 16$ with a step size 2 meters. The number of the iteration of the numerical beamforming method is set to be 10 in Figure 5.9. Clearly, we can observe that the closer the IRS to the BS, the more signal power can be received. This is matching our initial guess, since the IRS, which is a passive device, can receive more signal power with a large open angle from the BS. The same observation can be concluded from Figure 5.10, where the deploying position of the IRS is moving upwards to the north wall of the room.

However, if we deploy the IRS to close to the BS, such as $y_{irs} = 2$ or $y_{\text{irs}} = 4$, the performance of the IRS is not outstanding. This is because when the IRS is too close to the BS, the outgoing propagation angle from the BS is nearly 180°. There are some fluctuations when the material of the obstacle wall changes from low attenuation material to Concrete (attenuation loss is 35dB according to Table 5.1) even the number of the iteration increases to 30. This is because it is hard to optimize joint beamforming through the numerical beamforming method. IRS needs to support the valid transmission simultaneously between the BS and the user under their coverage region [6].

The threshold point of the user is defined as a position that when deploying position of IRS is entering the region that there is a LoS propagation between the IRS and the user, where that in Figure 5.9 is $y_{\text{irs}} = 8$. The user receives both non-LoS signal propagation from the BS and the IRS, and of course, we can see that the received signal power is quite low compared to that above the threshold point of the user. In Figure 5.8b, d_{th} denotes the vertical distance between the threshold position of the user and the origin point, and d_{LoS} denotes the horizontal distance between the threshold position of BS and the west wall where the threshold point of the BS is defined as a position that the farthest position the BS get cover on the north wall. Moreover, if we want to fully compensate for the attenuation loss caused by the obstacle wall, we need to adjust the deploying position of IRS such that there are more IRS elements placing above the threshold point. Furthermore, we need to consider the width of the IRS when we deploy it. Hence, the near-optimal performance of the received signal power of the user can be achieved when the IRS deploying position is slightly higher than the threshold point of the user.

Figure 5.10 presents the relationship between the size of the IRS and the received signal power for different IRS deploying position and different obstacle materials, where the IRS deploying position varies from $y_{\text{irs}} = 25$ to $y_{\text{irs}} = 45$ with 5 meters

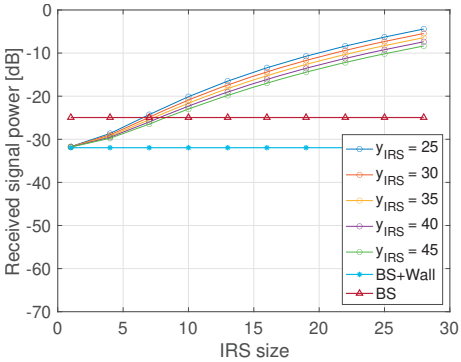

(a) Glass window (7dB attenuation)

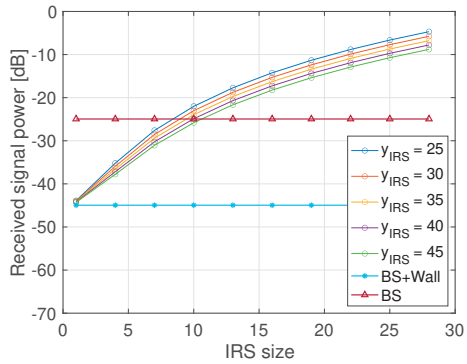

(b) Brick wall 1 (120mm) (20dB attenuation)

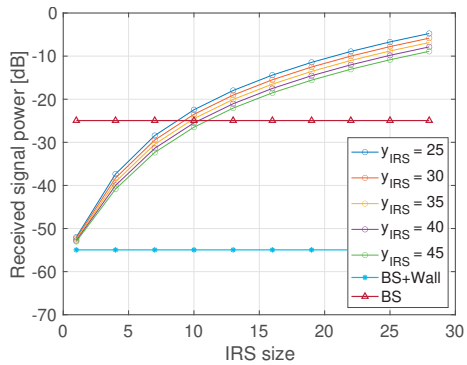

(c) Armored glass (30dB attenuation)

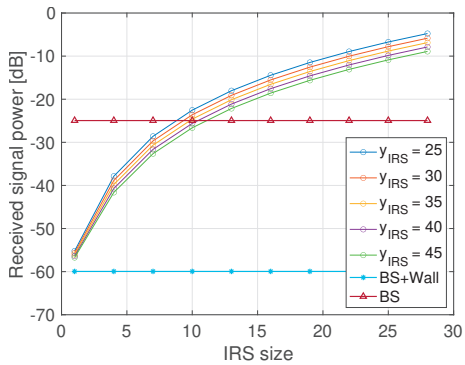

(d) Concrete (35dB attenuation)

Figure 5.10: Relationship between size of the IRS (side length M) and received signal power for four different wall loss attenuation and different IRS deploying positions from $y_{\text{irs}} = 25$ to $y_{\text{irs}} = 45$ on the west wall when L=8.

step size between each simulation. As we deploy the IRS above the threshold point of the user ($d_{\text{irs}} > d_{\text{th}}$), the received signal power decreases linearly when the IRS is moving upward to the north wall. The received signal power has a better performance when $y_{\text{irs}} = 25$ for all materials.

Figure 5.11 shows the relationship between the deploying position in the y-axis and the power compensation size of the IRS with different attenuation loss due to different obstacle materials. We remain the same geometric and antenna setting as the one used in Figure 5.9 and Figure 5.10. The number of the IRS size which can compensate for the attenuation loss increases as the deploying position of the IRS moving upwards in the y-axis. We can apply the minimum size of the IRS and deploy it around the threshold point in order to improve the energy consumption. Since the size of the IRS has to be a "whole number", the size of

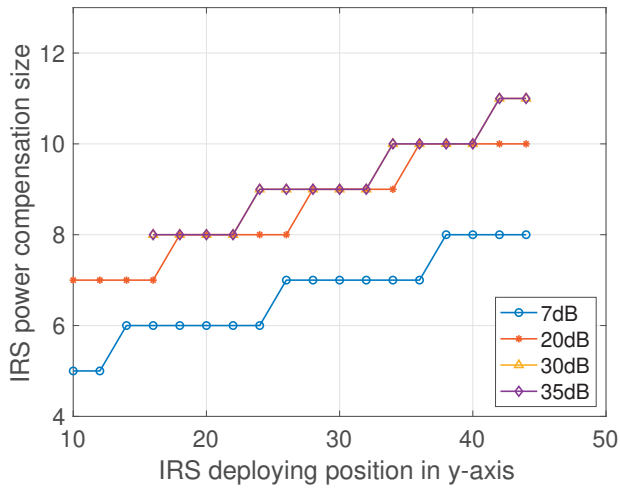

Figure 5.11: Relationship between minimum IRS sizes that can compensate for the attenuation loss and its corresponding deploying position along the y-axis with four different attenuation loss when $L = 8$ and $l_2 = 20m$.

the IRS size which can compensate for the attenuation loss is the same within a certain range and then increase as the deploying position moving the north wall of the room. Overall, the shape of the IRS power compensation size is shifting to the top as well as to the right when the attenuation loss from the obstacle is increasing, and the size is increase by 3 measured from the minimal size point for all attenuation loss listed in the figure. The IRS compensation size of the concrete wall (with 30dB attenuation loss) is overlap with that of the armored glass (with 35dB attenuation loss). The minimal IRS compensation sizes of the glass wall (7dB attenuation loss) and the brick wall 1 (20dB attenuation loss) occurs when the IRS at $y_{\text{irs}} = 10$ with size 5 and 7 respectively, while that sizes of the concrete wall and the armored glass are starting from $y_{\text{irs}} = 16$ with size 8. It can be observed that when the attenuation loss increase by 10dB, the corresponding IRS power compensation size roughly increases by one. For instance, the IRS compensation size for 20dB attenuation is roughly one size smaller than that for 30dB attenuation with the same y_{irs}.

In Figure 5.12, the vertical distance between the obstacle wall and the south wall is increase to $l_2 = 30$ and we keep the same geometric setups as in Figure 5.11. Since l_2 is increased, the corresponding threshold position is also moving upward along the y-axis. This causes the number of the minimum IRS size to increase accordingly. Comparing the results shown in Figure 5.11, the IRS compensation size is varying within 2dB for all attenuation loss listed in the figure. It can be observed that the minimal IRS compensation size for 7dB, 30dB, and 35dB attenuation loss is starting at the same number with size 9.

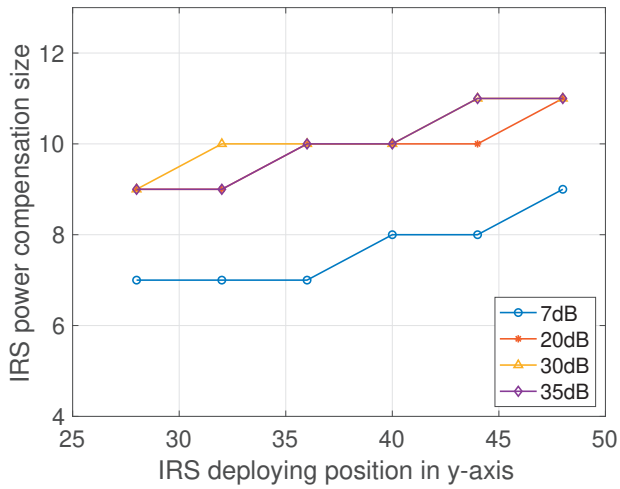

Figure 5.12: Relationship between minimum IRS sizes that can compensate for the attenuation loss and its corresponding deploying position along the y-axis with four different attenuation loss when $L = 8$ and $l_2 = 30m$.

Second, we discuss the power performance of the scenario which shown in Figure 5.13, where an IRS is deployed along the north wall. Figure 5.13a presents the detail geometric setups with wireless channel information, while Figure 5.13b provides a clear view of the BS and the user's coverage region.

Figure 5.14 presents the relationship between the size of the IRS and the received signal power for different IRS deploying positions on the north wall. The red triangular dot line denotes the received power of the user when the room is empty without any obstacle blocking the user from the BS, and the bottom blue triangular dot line denotes the received power of the user when there is an office wall blocking the direct link between the base station and the user, while the curves between them denote the corresponding received power of the user with different IRS deploying position when there is an office wall blocking the direct link between the base station and the user. The threshold position of BS is $d_{\text{LOS}} = 22.5m$ when $l2 = 20$. Similar reason for deploying on the west wall, if the IRS deploying across the threshold position of the BS, the direct propagation link between the IRS and the BS will be blocked by the obstacle. Since the IRS is a passive device, therefore, the signal received by the user is reduced significantly and the size of the IRS which can compensate for the attenuation loss will be increase greatly. Hence, we only focus on deploying the IRS left to the threshold position of the BS on the north wall ($d_{\text{irs}} < d_{\text{LoS}}$).

The deploying position of the IRS is moving along with the yellow line shown

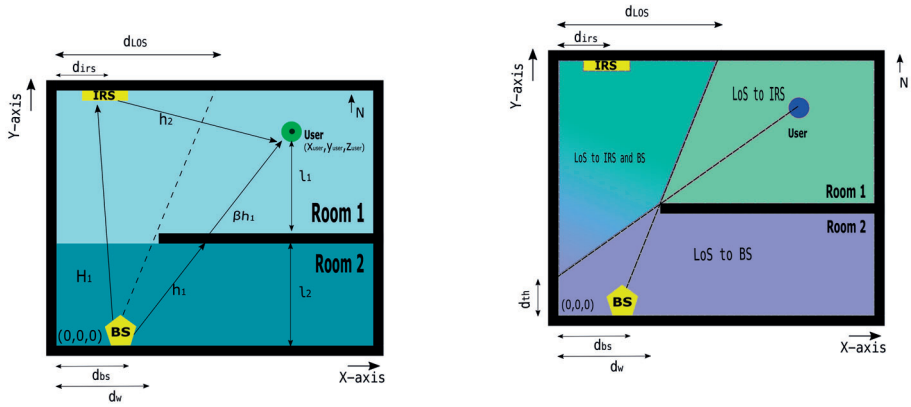

(a) Wireless channel perspective

(b) Signal coverage perspective (From User point of view)

Figure 5.13: Vertical views of the Dead-Zone power compensation scenario geometric setup where IRS is placed on the north wall.

in Figure 5.13b, where it varies from $x_{\text{irs}} = 0$ to $x_{\text{irs}} = 20$ with a step size 5 meters. To get a better system performance, the number of the iteration of the numerical beamforming method is set to be 10 in Figure 5.14. Overall, the received signal power of the user is increasing linearly as the IRS moving to the right. The best deploying position for an IRS is located at the threshold position when $d_{\text{irs}} = d_{\text{LoS}}$. This is because the IRS is deploying at the region that is LoS to the BS. In practice, we have to consider the width of the IRS. Hence, the near-optimal performance of the received signal power of the user can be achieved when the IRS deploying position is slight to the left of the threshold point of the BS.

Figure 5.15 illustrates the relationship between the IRS size which can compensate for the attenuation loss and the IRS deploying position along x-axis when $L = 8$ and $l_2 = 20m$ with 4 different material of the obstacle wall. Overall, the size different between different attenuation loss are smaller than that in the Figure 5.11. Comparing with Figure 5.11 where L=8 and $l_2 = 20m$, the minimum IRS size that compensated the attenuation loss is much larger when the deploying position is close to the threshold point of the BS. When we increase l_2, the threshold point will move towards to the west wall, and therefore, it can be predicted that the results will be even worse than that when $l_2 = 30m$.

5.3 Power VS travel distance

In Section 5.2, the received signal power behavior and the power compensation

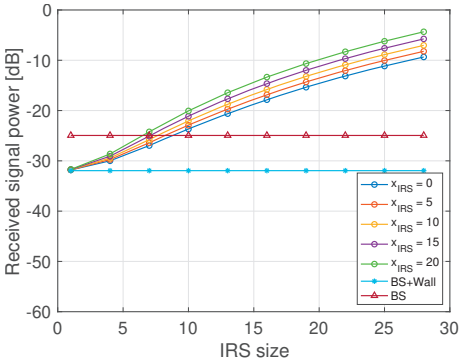

(a) Glass window (7dB attenuation)

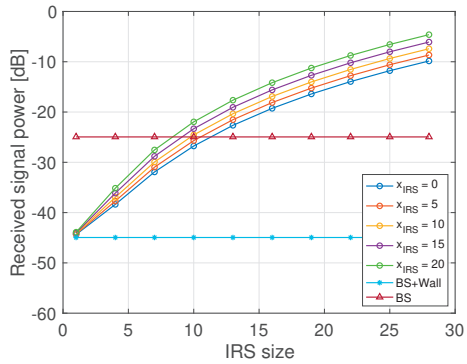

(b) Brick wall 1 (120mm) (20dB attenuation)

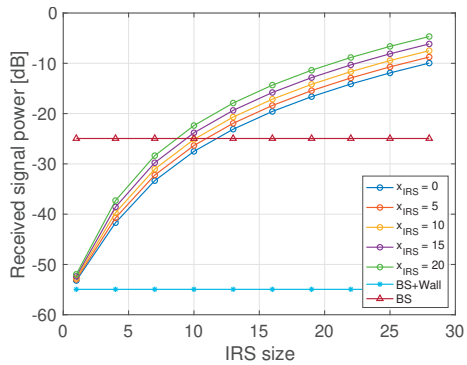

(c) Armored glass (30dB attenuation)

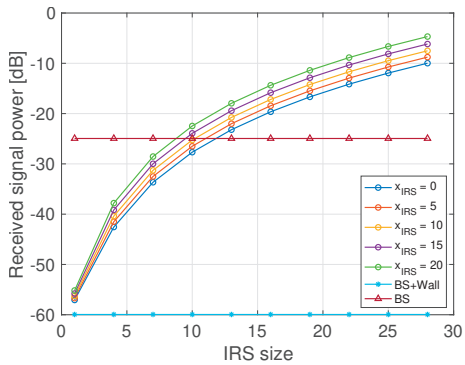

(d) Concrete (35dB attenuation)

Figure 5.14: Relationship between size of the IRS (side length M) and received signal power for four different wall loss attenuation and different IRS deploying positions from $x_{\text{irs}} = 0$ to $x_{\text{irs}} = 20$ on the west wall when $L = 8$.

size with respect to the IRS deployment position in the Dead-Zone scenario are elaborated. While the total distance in the x-y plane between the IRS and the BS, and between the IRS and the user keeps varying during the simulation. In this section, we are interested in analyzing the received signal power behavior when we fix the total travel distance. The travel distance of the user and the BS are denoted d_{u} and d_{b}, respectively, and the total travel distance is the sum of the d_{u} and d_{b} which denotes as d_{total}. All the travel distance is measured in the x-y plane in 2D and we do not consider the height of each element in this section. The geometric setup of the corresponding scenario is shown in Figure 5.16. An IRS is deployed at the origin position, and we assume that all elements from the IRS are entirely exposed to the user and the BS. The user is moving along the dotted line in space 1 with a travel angle θ_{u}, while the BS the moving along the dot line in space 2 with a travel angle θ_{b}. In particular, we assume there is no direct propagation link between the BS and the user in the entire movement, where the link is

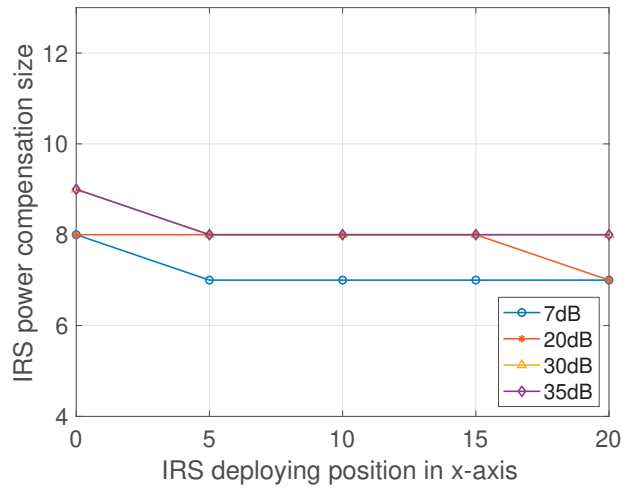

Figure 5.15: Relationship between the minimum IRS sizes that can compensate for the attenuation loss and its corresponding deployment position along the x-axis with four different attenuation loss when L=8 and $l_2 = 20m$.

fully blocked by the obstacle lain in between. Hence, the entire open space can be divided equally into two subspace, Space 1 and Space 2, which can be described as the LoS to the user region and the LoS to the BS region, respectively.

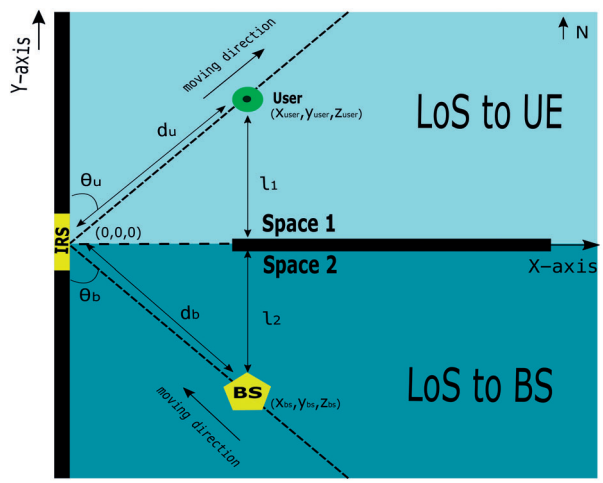

Figure 5.16: The geometric setup of power VS travel distance.

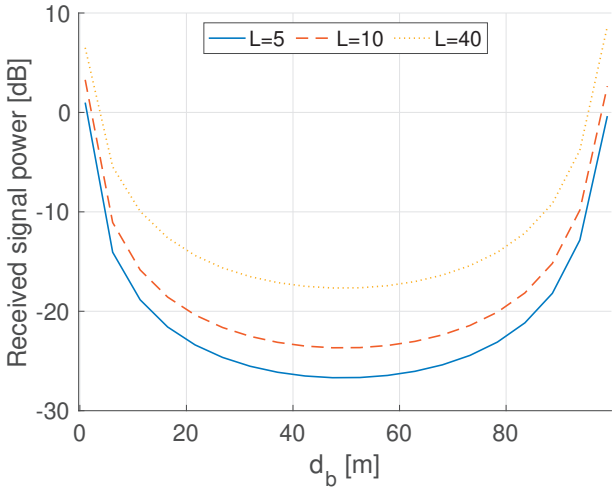

Figure 5.17: Relationship between received signal power of the user and user travel distance for different number of antennas at the BS when $M = N = 13$ and $\theta_{\mathrm{u}} = \theta_{\mathrm{b}} = 45°$.

In Figure 5.17, we compare the received signal power of the user versus the user travel distance for different numbers of the antenna at the BS when $M = N = 13$, and $\theta_{\mathrm{u}} = \theta_{\mathrm{b}} = 45°$. We set d_{b} is changing linearly from 1m to 100m. Overall, as the number of antennas at the BS increases, the received signal power increases. For example, when $d_{\mathrm{b}} = 50m$, the received signal power for $L = 10$ is around 3dB larger than that for $L = 5$, and is around 6dB smaller than that for $L = 40$. This is because increasing L enables more IRS elements to receive the signal energy from the BS which results in an array gain of L [5]. It can be observed that the received signal power is much higher when either the BS or the user is closed to the passive IRS, and the received signal power is lower when neither of them close to the IRS.

Figure 5.18 presents the relationship between the received signal power of the user and user travel distance for different number of the antenna elements at the IRS when $\theta_{\mathrm{u}} = \theta_{\mathrm{b}} = 45°$. The total travel distance d_{total} is 100m and we vary the number of antenna elements at the IRS from size 10 to 20 in this case. Overall, the curves behave similarly as the one shown in Figure 5.17, while offset difference is around 12dB. This is because the IRS is comprised of M by N reflective antenna elements thus a total reflected beamforming gain from the IRS becomes $(M \times N)^2$ [5].

In Figure 5.19 and Figure 5.20, we compare the received signal power with different user travel angles versus the travel angel of the user (θ_{u}) and the travel angel of the BS (θ_{b}), respectively, when $L = 10$ and $M = N = 13$. Overall, neither θ_{b} and θ_{u} influence the behavior of the received signal power, and the shape of the

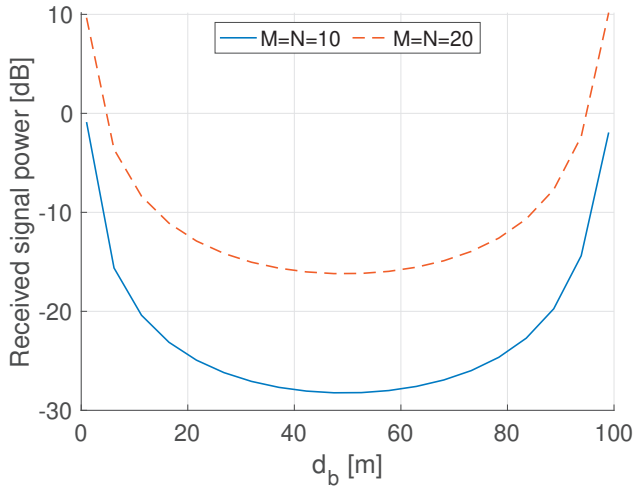

Figure 5.18: Relationship between received signal power of the user and user travel distance for different IRS size when $L = 10$ and $\theta_{\mathrm{u}} = \theta_{\mathrm{b}} = 45^{\circ}$.

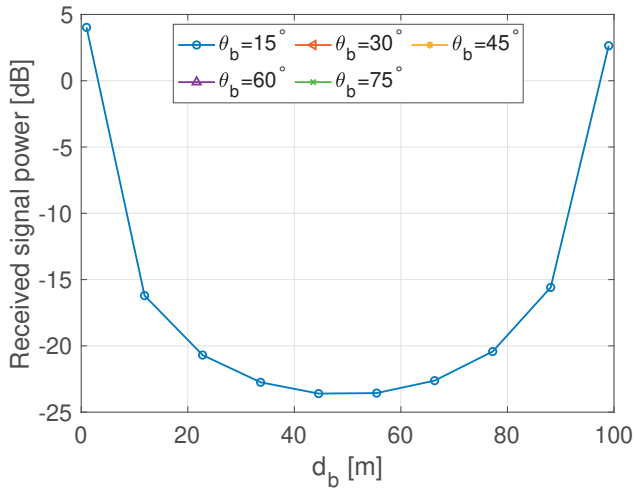

Figure 5.19: Relationship between received signal power of the user and user travel distance for different θ_{u} when $L = 10$, $M = N = 13$, and $\theta_{\mathrm{u}} = 45^{\circ}$.

figure is same as the one shown Figure 5.17. This is because the transmit-MRC optimizes the beamforming of the antennas at the base station, such that the output beams are directed to the IRS. The same reason for the wireless link between the IRS and the user, the numerical beamforming optimization is robust such that the results are not affected by the steering angels. Since we can not control the

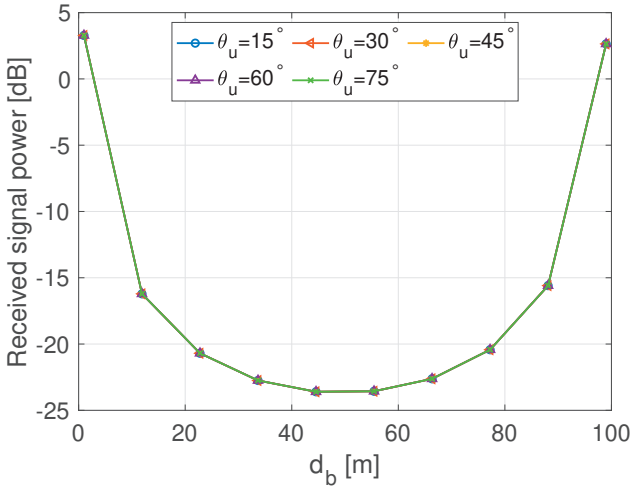

Figure 5.20: Relationship between received signal power of the user and user travel distance for different θ_{b} when $L = 10$, $M = N = 13$, and $\theta_{\mathrm{b}} = 45°$.

movement of the user, we need to deploy the BS closer to the IRS such that d_{u} is closed to the corresponding position of the right peak with a smaller θ_{b}.

Chapter 6

Conclusion and Future Works

6.1 Conclusion

In this thesis, an approach to improving wireless networks' performance by deploying passive IRSs is proposed. The signal model and the beamforming algorithm of the MISO wireless communication system have been built and discussed in Section 3 and Section 4. Precisely, the transmit-MRC beamforming at the BS and the passive reflect beamforming of the phase shifters at the IRS are jointly optimized to maximize the signal power received at the user in an IRS-aided MISO system. From simulation results, we provide an overview of the IRS-aided wireless network performance in three different scenarios, including Empty-Room, Dead-Zone, and Power VS travel distance, respectively. Moreover, we compare the IRS power compensation size versus the IRS deploying position in the x-axis and y-axis. Simulation results show that the optimized solution of the IRS deploying position is to deploy the IRS as close as the threshold point of the BS or the user, such that to compensate for the power attenuation caused by the obstacle. In other words, the received signal power behaves oppositely as the IRS moves away from the threshold point. In practice, the minimum number of the IRS elements can be chosen depending on the IRS's deployment position. Furthermore, we compare the received signal power versus the user travel distance with different travel angels for an open space setup and the movement shown in Figure 5.16. Interestingly, it was shown that the optimal received signal power is not affected by travel angles, and it can be achieved when either the base station or the user is closed to the IRS.

6.2 Future Work

In practice, the propagation environment may be complicated and each IRS can be associated with multiple BSs. In such scenarios, using such a method discussed above alone for deploying IRS may be ineffective. Finding the optimal location requires global CSI at all locations, which is practically difficult to obtain. For future work, an interesting search topic on achieving autonomous de-

ployment of IRSs to predict the most suitable locations is a new problem of high practical interest.

References

[1] S. Hu, F. Rusek and O. Edfors, "The Potential of Using Large Antenna Arrays on Intelligent Surfaces," 2017 IEEE 85th Vehicular Technology Conference (VTC Spring), Sydney, NSW, 2017, pp. 1-6, doi: 10.1109/VTCSpring.2017.8108330.

[2] T. L. Marzetta, "Noncooperative Cellular Wireless with Unlimited Numbers of Base Station Antennas," in IEEE Transactions on Wireless Communications, vol. 9, no. 11, pp. 3590-3600, November 2010.

[3] F. Rusek et al., "Scaling Up MIMO: Opportunities and Challenges with Very Large Arrays," in IEEE Signal Processing Magazine, vol. 30, no. 1, pp. 40-60, Jan. 2013.

[4] E. G. Larsson, O. Edfors, F. Tufvesson and T. L. Marzetta, "Massive MIMO for next generation wireless systems," in IEEE Communications Magazine, vol. 52, no. 2, pp. 186-195, February 2014.

[5] Q. Wu and R. Zhang, "Intelligent Reflecting Surface Enhanced Wireless Network: Joint Active and Passive Beamforming Design," 2018 IEEE Global Communications Conference (GLOBECOM), Abu Dhabi, United Arab Emirates, 2018, pp. 1-6.

[6] Q. Wu and R. Zhang, "Intelligent Reflecting Surface Enhanced Wireless Network via Joint Active and Passive Beamforming," in IEEE Transactions on Wireless Communications, vol. 18, no. 11, pp. 5394-5409, Nov. 2019.

[7] C. Huang, A. Zappone, G. C. Alexandropoulos, M. Debbah and C. Yuen, "Reconfigurable Intelligent Surfaces for Energy Efficiency in Wireless Communication," in IEEE Transactions on Wireless Communications, vol. 18, no. 8, pp. 4157-4170, Aug. 2019.

[8] E. Björnson, L. Sanguinetti, J. Hoydis and M. Debbah, "Designing multiuser MIMO for energy efficiency: When is massive MIMO the answer?," 2014 IEEE Wireless Communications and Networking Conference (WCNC), Istanbul, 2014, pp. 242-247.

[9] Q. Wu and R. Zhang, "Towards Smart and Reconfigurable Environment: Intelligent Reflecting Surface Aided Wireless Network," in IEEE Communications Magazine, vol. 58, no. 1, pp. 106-112, January 2020.

[10] B. Zheng and R. Zhang, "Intelligent Reflecting Surface-Enhanced OFDM: Channel Estimation and Reflection Optimization," in IEEE Wireless Communications Letters, vol. 9, no. 4, pp. 518-522, April 2020.

[11] C. Huang, G. C. Alexandropoulos, C. Yuen and M. Debbah, "Indoor Signal Focusing with Deep Learning Designed Reconfigurable Intelligent Surfaces," 2019 IEEE 20th International Workshop on Signal Processing Advances in Wireless Communications (SPAWC), Cannes, France, 2019, pp. 1-5.

[12] L. Lu, G. Y. Li, A. L. Swindlehurst, A. Ashikhmin and R. Zhang, "An Overview of Massive MIMO: Benefits and Challenges," in IEEE Journal of Selected Topics in Signal Processing, vol. 8, no. 5, pp. 742-758, Oct. 2014.

[13] C. Huang, A. Zappone, M. Debbah and C. Yuen, "Achievable Rate Maximization by Passive Intelligent Mirrors," 2018 IEEE International Conference on Acoustics, Speech and Signal Processing (ICASSP), Calgary, AB, 2018, pp. 3714-3718.

[14] L. Subrt and P. Pechac, "Intelligent walls as autonomous parts of smart indoor environments," in IET Communications, vol. 6, no. 8, pp. 1004-1010, 22 May 2012.

[15] S. V. Hum and J. Perruisseau-Carrier, "Reconfigurable Reflectarrays and Array Lenses for Dynamic Antenna Beam Control: A Review," in IEEE Transactions on Antennas and Propagation, vol. 62, no. 1, pp. 183-198, Jan. 2014.

[16] X. Tan, Z. Sun, J. M. Jornet and D. Pados, "Increasing indoor spectrum sharing capacity using smart reflect-array," 2016 IEEE International Conference on Communications (ICC), Kuala Lumpur, 2016, pp. 1-6.

[17] X. Tan, Z. Sun, D. Koutsonikolas and J. M. Jornet, "Enabling Indoor Mobile Millimeter-wave Networks Based on Smart Reflect-arrays," IEEE INFOCOM 2018 - IEEE Conference on Computer Communications, Honolulu, HI, 2018, pp. 270-278, doi: 10.1109/INFOCOM.2018.8485924.

[18] C. Liaskos et al., “Using any surface to realize a new paradigm for wireless communications,” 2018. [Online]. Available: http://arxiv.org/abs/1806.04585.

[19] L. Subrt and P. Pechac, "Controlling propagation environments using Intelligent Walls," 2012 6th European Conference on Antennas and Propagation (EUCAP), Prague, 2012, pp. 1-5.

[20] E. Basar, M. Di Renzo, J. De Rosny, M. Debbah, M. Alouini and R. Zhang, "Wireless Communications Through Reconfigurable Intelligent Surfaces," in IEEE Access, vol. 7, pp. 116753-116773, 2019.

[21] Q. Wu and R. Zhang, "Beamforming Optimization for Wireless Network Aided by Intelligent Reflecting Surface With Discrete Phase Shifts," in IEEE Transactions on Communications, vol. 68, no. 3, pp. 1838-1851, March 2020.

[22] Ericsson, "Beamforming,cell-centric to user-centric" from http://www.ericsson.com/en/network/trending/hot-topics/5g-radio-access/beamforming.

[23] RCRWirelessNews, "5G NR: Massive MIMO and Beamforming – What does it mean and how can I measure it in the field?" from https://www.rcrwireless.com/20180912/5g/5g-nr-massive-mimo-and-beamforming-what-does-it-mean-and-how-can-i-measure-it-in-the-field.

[24] Yuu-Seng Lau, Z. M. Hussain and R. J. Harris, "A weight-vector LMS algorithm for adaptive beamforming," 2004 IEEE Region 10 Conference TENCON 2004., Chiang Mai, 2004, pp. 495-498 Vol. 1.

[25] E.Björnson. 2018. Adaptive Beamforming and Antenna Arrays. http://ma-mimo.ellintech.se/2018/11/29/adaptive-beamforming-and-antenna-arrays/.

[26] A. A. Awan, Irfanullah, S. Khattak and A. N. Malik, "Performance comparisons of fixed and adaptive beamforming techniques for 4G smart antennas," 2017 International Conference on Communication, Computing and Digital Systems (C-CODE), Islamabad, 2017, pp. 17-20.

[27] S. Yong-jiang, Q. Dong-dong, R. Jia-ren, Z. Peng and D. R. Becerra, "Research on adaptive beamforming algorithm," 2012 International Conference on Image Analysis and Signal Processing, Hangzhou, 2012, pp. 1-3.

[28] A. Paulraj, R. Nabar, and D. Gore, *Introduction to space-time wireless communications*. Cambridge university press, 2003.

[29] Wikipedia,"Precoding", https://en.wikipedia.org/wiki/Precoding.

[30] H. Weingarten, Y. Steinberg and S. S. Shamai, "The Capacity Region of the Gaussian Multiple-Input Multiple-Output Broadcast Channel," in IEEE Transactions on Information Theory, vol. 52, no. 9, pp. 3936-3964, Sept. 2006.

[31] T. K. Y. Lo, "Maximum ratio transmission," in IEEE Transactions on Communications, vol. 47, no. 10, pp. 1458-1461, Oct. 1999.

[32] M. Joham, W. Utschick and J. A. Nossek, "Linear transmit processing in MIMO communications systems," in IEEE Transactions on Signal Processing, vol. 53, no. 8, pp. 2700-2712, Aug. 2005, doi: 10.1109/TSP.2005.850331.

[33] M. Joham, W. Utschick and J. A. Nossek, "Linear transmit processing in MIMO communications systems," in IEEE Transactions on Signal Processing, vol. 53, no. 8, pp. 2700-2712, Aug. 2005.

[34] Y. Jin and X. Xia, "An Interference Nulling Based Channel Independent Precoding for MIMO-OFDM Systems with Insufficient Cyclic Prefix," in IEEE Transactions on Communications, vol. 61, no. 1, pp. 131-143, January 2013.

[35] X. Feng and C. Leung, "A new optimal transmit and receive diversity scheme," 2001 IEEE Pacific Rim Conference on Communications, Computers and Signal Processing (IEEE Cat. No.01CH37233), Victoria, BC, Canada, 2001, pp. 538-541 vol.2.

[36] A. Díaz-Rubio, V. Asadchy, A. Elsakka and S. Tretyakov, "Metasurfaces for perfect control of reflection," 2017 International Workshop on Antenna Technology: Small Antennas, Innovative Structures, and Applications (iWAT), Athens, 2017, pp. 3-5.

[37] Huawei, *FAQ-How Much Is the Attenuation of Typical Obstacles*, from `https://support.huawei.com/enterprise/en/knowledge/KB1000079516/?idAbsPath=7919710$%$7C21782164%7C21782201%7C22318535%7C21560861`.

Printed by Tryckeriet i E-huset, Lund 2021

LUND
UNIVERSITY

Series of Master's theses
Department of Electrical and Information Technology
LU/LTH-EIT 2021-811
http://www.eit.lth.se